PCCP

Accepted Manuscript

ROYAL SOCIETY OF CHEMISTRY

www.rsc.org/pccp

Tuning the reactivity of a dissociative force field: proton transfer properties of aqueous H_3O^+ and their dependence on the three–body interaction.

Martin J. Wiedemair, Manuel Hitzenberger and
Thomas S. Hofer[*]

Theoretical Chemistry Division
Institute of General, Inorganic and Theoretical Chemistry
University of Innsbruck, Innrain 80-82, 6020 Innsbruck, Austria
E-Mail: t.hofer@uibk.ac.at
Tel.: +43-512-507-57111
Fax: +43-512-507-57199

March 17, 2015

[*]Corresponding author

Abstract

The proton transfer properties of the dissociative water potential developed by Garofalini *et al.* were closely examined by carefully analyzing the pairwise screening functions of the three-body interaction. It was shown that a simultaneous adjustment of the exponential screening factor and the three-body cutoff distance enables a selective adjustment of the diffusive properties of an excess proton, while at the same time structural and other dynamical data remains unaffected to a large extend.

To investigate proton transfer properties without the influence of nuclear quantum effects, deuterated systems have been investigated in addition to their hydrogen counterparts. It was shown that the suggested parameter set A leads to significantly improved diffusion coefficients and proton hopping rates. Comparison of proton transfer correlation functions to simulation data obtained from Car-Parrinello molecular dynamics simulations confirms the improved performance of the adjusted parametrization.

Introduction

As a consequence of the continuously increasing capacities of modern computational infrastructure, theoretical approaches in science and engineering have become an important complement to experimental investigations. Among the broad field of applications simulations of molecular systems have become an indispensable tool in chemical research, which was recently acknowledged by the awarding of the Nobel prize to Martin Karplus, Michael Levitt and Arieh Warshel *"for the development of multiscale models for complex chemical systems"*[1].

Quantum mechanical (QM) techniques[2,3,4] are employed as general and accurate approaches for the description of the electronic structure of atoms and molecules, but are also known for their high computational demand, limiting the range of applications to comparably small system sizes. On the other hand the description of a chemical system based on a molecular mechanical (MM) formulation proved as a fast, flexible and versatile approach[5,6,7]. These empirical methods, also referred to as force fields, utilize pre-parametrized potential functions, typically focused on a particular class of chemical systems, as for example peptides and nucleic acids[8,9,10,11,12,13,14], minerals[15] or ionic liquids[16,17,18].

In order to achieve an efficient yet accurate representation of chemical interactions, a number of approximations have to be made. Typically, intermolecular contributions are treated based on a Coulombic plus non-Coulombic interactions, the latter often being modeled via a Lennard-Jones potential[19,20]. To describe intramolecular degrees of freedom harmonic bond and angle formulations plus cosine-based dihedral expressions are employed. Despite providing an adequate compromise between computational demand and accuracy of results, the use of the harmonic approximation imposes a rather severe restriction, namely the inability to describe the cleavage and formation of chemical bonds. Particle pairs defined as bonded in the initial configuration will remain bonded throughout the

entire simulation, while particles not defined as bonded are prevented from forming a bond, even if a chemical process would require them to do so.

This restriction does not apply to all force field formulations and the development of reactive force field approaches, *i.e.* potentials enabling a topology change in the course of a simulation, received increased interest during the last years[21,22,23,24]. In order to achieve a dissociative description of chemical processes via force fields, the distinction between intra- and intermolecular contributions has to be abandoned, since an initially bonded particle pair may not form a bond at later stages of a simulation and *vice versa*. Such a formulation is for instance realized in the central force water model derived by Stillinger and coworkers[25,26,27]. Altough not explicitly parametrized for the description of proton transfer (PT) events in liquid water, this model does in principle enable changes of the chemical topology. Other dissociative potentials for water have been presented by Billeter and van Gunsteren[28,29], Ojamäe *et al.* (sOSS2),[30,31] Hofmann *et al.*[22] and Wolf and Groenhof[32]. A further widely employed method to model chemical reactions via potential functions is based on the empirical valence bond (EVB) approach introduced by Warshel and Weiss[33]. In this method the electronic state of a particular configuration is represented as superposition of states, which are modeled via empirical potentials. Today multi-state (MS) EVB techniques are widely employed in studies of excess protons[34,35,36,37,38,39,40] as well as hydroxide[41] in aqueous solution.

The potential model developed by Mahadevan and Garofalini[23] was shown to be capable of describing proton transfer reactions between water, oxonium and hydroxide in aqueous solution as well as accurately reproducing structural properties, vibrational frequencies, the liquid–vapor coexistence curve and the temperature-pressure relation of pure water. Due to its functional form it also enables a straightforward application in hybrid quantum mechanical/molecular

mechanical (QM/MM) simulation studies[42,43]. Despite the accurate description of liquid water by the Garofalini model, the prediction of the diffusion coefficient of the excess proton and the associated average proton hopping rate, determined as 0.38 Å^2/ps and 0.25 ps^{-1} [42], show a rather large deviation from the experimental value reported as 0.93 Å^2/ps[44,45] and 0.75 ps^{-1} [46], respectively.

Thus, the main target of this work was to identify and adjust the force field parameters governing proton transfer properties of an aqueous excess proton without altering other structural and dynamical properties predicted by the model. In the next section methodical details and the parametrization strategy are outlined, followed by a discussion of structural and dynamical properties obtained for the modified model and concluding remarks.

Methods

Simulation method

In order to achieve a dissociative description of a system, no distinction between intra- and intermolecular interactions is made. Novel dissociative force field approaches like the one developed by Mahadevan and Garofalini[23] apply the same potential to a respective atom pair (*e.g.* O-H), irrespective of the chemical topology (*i.e.* bonded or non-bonded). In addition, each atom in the system is represented as a pointcharge surrounded by a Gaussian charge cloud with opposite sign, both centered at the nucleus. The corresponding two-body potential is given as

$$U_{2bd} = U_{qq} + U_{q^d q^d} + U_{qq^d} + U_{q^d q} + U_{rep} + U_{disp} \tag{1}$$

with q and q^d denoting the pointcharges and diffuse Gaussian charge distributions, respectively. The first four contributions to the pair potential represent

Coulombic terms, accounting for all interactions between pointcharges and Gaussian charge clouds of a particular particle pair. The last two terms account for repulsive and dispersive non-Coulombic terms, respectively.

In addition, the model includes a screened, cosine-harmonic three-body term U_{3bd} applied to all H-O-H angles, irrespective whether the atoms are part of a molecular unit (water, oxonium, hydroxide) or not.

$$U_{3bd}\left(\mathbf{r}_{ij},\mathbf{r}_{ik},\theta_{jik}\right) = \lambda_{jik} e^{\frac{\gamma_{ij}}{\|\mathbf{r}_{ij}\|-r_{ij}^0}} e^{\frac{\gamma_{ik}}{\|\mathbf{r}_{ik}\|-r_{ik}^0}} \left[cos\left(\theta_{jik}\right) - cos\left(\theta_{jik}^0\right)\right]^2 \quad (2)$$

$$= k_{\text{eff}} \left[cos\left(\theta_{jik}\right) - cos\left(\theta_{jik}^0\right)\right]^2 \quad (3)$$

Here, $\mathbf{r}_{ij}$, $\mathbf{r}_{ik}$ and θ_{jik} correspond to the pair vectors and the angle of a particle triple $j-i-k$. The equilibrium angle θ_{jik}^0 was set in such a way that together with the H-H pair interaction the equilibrium H-O-H angle of an isolated water molecule adopts an ideal value of 104.2°. The exponentially decaying screening functions eliminate the contribution of this angle potential whenever one of the pair distances $\mathbf{r}_{ij}$ and $\mathbf{r}_{ik}$ are beyond the respective cutoff distance r_{ij}^0 and r_{ik}^0, respectively. The magnitude of this screening is controlled by the exponential factors γ_{ij} and γ_{ik}. The prefactor λ_{jik} has been adjusted so that its product with both screening functions yields an effective force constant k_{eff} for distances of $\mathbf{r}_{ij}$ and $\mathbf{r}_{ik}$, corresponding to the average O-H bond distance of a water molecule in aqueous solution (approximately 0.985 Å).

This description facilitates the formation and cleavage of O-H bonds along a simulation, thus enabling investigations of proton transfer reactions in systems containing excess protons as well as hydroxide ions. Since compatible parameters for sodium(I) and chloride ions have been reported as well[47], simulations of HCl and NaOH at different concentrations (*i.e.* pH values) are possible.

However, as mentioned earlier, the diffusion coefficient D and proton hopping rate h of an excess proton show a rather large deviation from experiment. Since proton transfer reactions are strongly dependent on the local environment, it can be expected that the parametrization of the three–body potential, in particular the exponential screening functions, have a strong influence on the proton transfer properties, as will be discussed in the following.

Parametrization

Due to the presence of the screening functions, the force contributions resulting from the three-body potential include, in addition to the perpendicular forces of the derivative of the cosine-harmonic expression, contributions resulting from the derivative of the exponential screening functions. For example the derivative with respect to the postion of particle j yields:

$$
\begin{aligned}
-\frac{\partial U_{3bd}}{\partial \mathbf{r}_j} =& 2\lambda_{jik} e^{\frac{\gamma_{ij}}{\|\mathbf{r}_{ij}\|-r_{ij}^0}} e^{\frac{\gamma_{ik}}{\|\mathbf{r}_{ik}\|-r_{ik}^0}} \left[cos\big(\theta_{jik}\big) - cos\big(\theta_{jik}^0\big)\right] \left[cos\big(\theta_{jik}\big)\frac{\mathbf{r}_{ij}}{\|\mathbf{r}_{ij}\|^2} - \frac{\mathbf{r}_{ik}}{\|\mathbf{r}_{ij}\|\|\mathbf{r}_{ik}\|}\right] + \\
& \lambda_{jik} e^{\frac{\gamma_{ij}}{\|\mathbf{r}_{ij}\|-r_{ij}^0}} e^{\frac{\gamma_{ik}}{\|\mathbf{r}_{ik}\|-r_{ik}^0}} \left[cos\big(\theta_{jik}\big) - cos\big(\theta_{jik}^0\big)\right]^2 \frac{\gamma_{ij}}{\big(\|\mathbf{r}_{ij}\| - r_{ij}^0\big)^2} \frac{\mathbf{r}_{ij}}{\|\mathbf{r}_{ij}\|} \qquad (4) \\
=& \mathbf{F}_j^{\alpha} + \mathbf{F}_j^{scr} \qquad (5)
\end{aligned}
$$

While the first contribution $\mathbf{F}_j^{\alpha}$ (*cf.* fig. 1a) acts perpendicular to the bond vector $\mathbf{r}_{ij}$ (and $\mathbf{r}_{ik}$ for the derivative of $\partial U_{3bd}/\partial \mathbf{r}_k$), the latter $\mathbf{F}_j^{scr}$ resulting from the derivative of the pairwise screening functions yields forces parallel to the bond (*cf.* fig. 1b). Due to the quadratic form of the cosine-harmonic expression, these parallel forces always act repulsive on a short length scale within the respective cutoff distances r_{ij}^0 and r_{ik}^0. Protons approaching an acceptor water molecule are subject to two three-body interactions stemming from the H-O-H interactions with

both water hydrogen atoms. Therefore, a strong dependence of the proton transfer characteristics on the properties of the three-body potential can be expected. Modification of the three-body potential offers the possibility to adjust the proton transfer properties without influencing the sensitive long-ranged pairwise contributions, thus providing an efficient parametrization strategy to selectively influence the proton transfer properties.

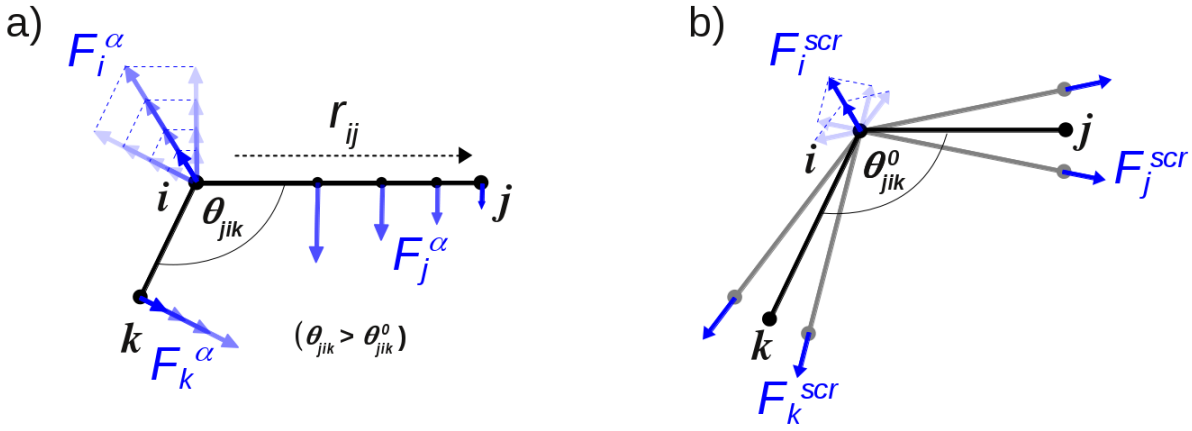

Figure 1: Force contributions for a particle triple $j - i - k$ resulting from the derivative of a) the angular component and b) the screening component of the three–body potential U_{3bd}. Due to the presence of the screening function all force contributions vanish upon increase of at least one of the pair distances. The forces resulting from the derivation of the screening functions $\mathbf{F}^{scr}$ always act repulsive, irrespective of whether the angle θ_{jik} is larger or smaller than the equilibrium value θ_{jik}^0.

Preliminary tests changing the prefactor λ_{jik} and/or the exponential factors γ proved unsuccessful, since this alters the effective force constant k_{eff} of the model (data not shown). In order to ensure that k_{eff} remains unchanged, the screening functions have to adopt the same value for the equilibrium O-H distance $\bar{r}_{OH}$ of 0.985 Å as shown in figure 2. This can be achieved for instance via a simultaneous adjustment of the cutoff distance r^0 and the γ parameter. Four different parameter sets labeled A to D and summarized in table 1 have been considered in this study, with set C corresponding to the original parametrization [23]. It is

interesting to note that a decrease of r^0 requires a decrease of γ to obtain the same value of the screening function for $\bar{r}_{OH}$ thus ensuring that k_{eff} is preserved for all parametrizations.

In addition to a change of the range of the three-body potential, the change of the r^0 and γ parameters has a strong influence on the force acting on a transferring proton. For example in case of the steepest parameter set A the increased slope near the equilibrium bond distance $\bar{r}_{OH}$ results in a larger repulsive force, which can be expected to lead to an increased probability of initiating PT events in an H_3O^+ ion. On the other hand, for distances close to the cutoff r_0 the slope is lower compared to the original parametrization. Transferring protons are subject to reduced repulsive forces when entering the cutoff range of an acceptor molecule. Thus, it can be expected that for parameter sets A and B, having a lower cut-off distance r_0 compared to the original set, the occurrence of PT reactions is increased, whereas the opposite trend can be expected for set D.

In order to investigate the influence of the different parametrizations on the PT properties, MD simulations of hydrochloric acid in light as well as in deuterated water have been carried out. After identifying an adequate parameter set, structural and dynamical properties of the solutions have been compared to the original parametrization of the model.

Set	r^0_{ij}	γ_{ij}
A	1.50	1.089
B	1.55	1.194
C	1.60	1.300
D	1.65	1.406

Table 1: Employed parameter sets used in this work in Å. The parameters have been adjusted to yield the same potential at the intramolecular OH equilibrium distance of 0.985 Å. Parameter set C corresponds to the original coefficients given by Mahadevan and Garofalini.[23]

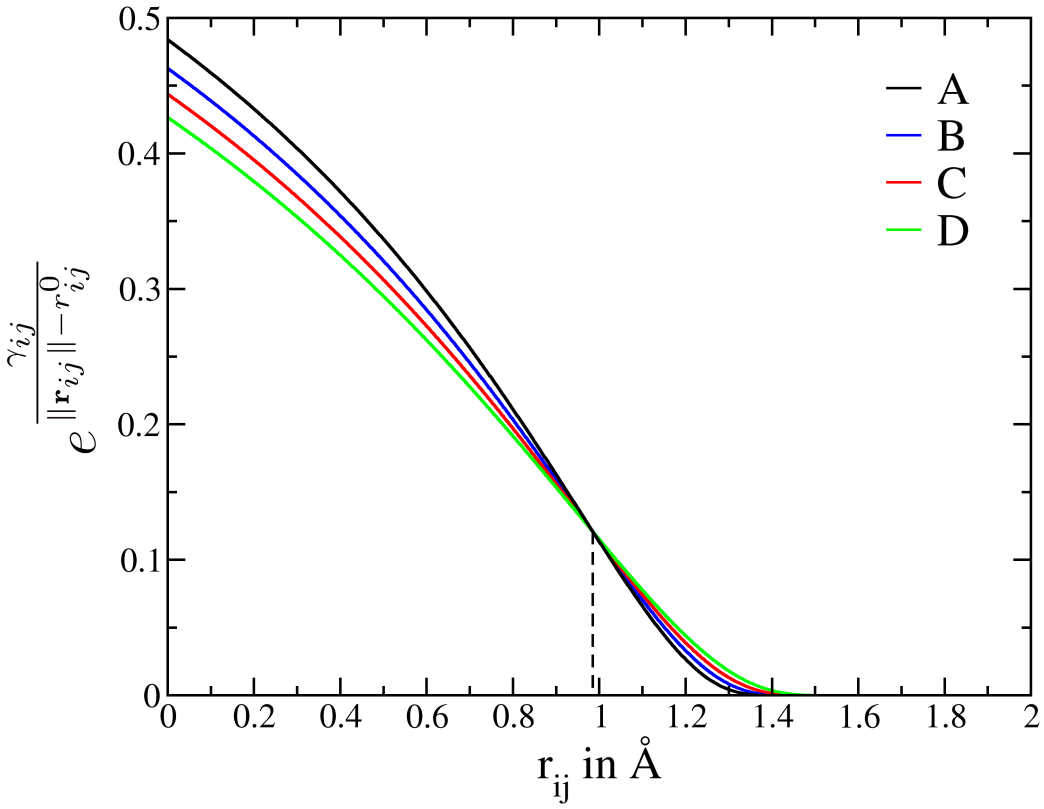

Figure 2: Influence of the different parametrizations on the screening function. The parameters have been adjusted to yield the same potential at the intramolecular OH equilibrium distance of 0.985 Å determined for the original parameter set C. Thus, the effective force constant k_{eff} for a water molecule remains unaffected to a large extend.

Simulation protocol

The starting structure for the performed simulations was derived from an earlier, similar run. Hofer *et al.*[42] worked with a periodic, cubic simulation box containing 17 HCl molecules and 1000 water molecules, which yields a 1M solution. To create a starting structure for this work's simulations, 16 of these HCl molecules were deleted resulting in a starting structure containing 1 Cl^-, 1 H_3O^+ and 999 water

molecules. An additional simulation box was created by replacing each Hydrogen (^{1}H) atom with a Deuterium (^{2}H) atom. The velocity-Verlet algorithm has been employed to integrate the equations of motion with a timestep of 0.2 fs. To account for long-range Coulombic interactions, the Wolf summation technique[48] with a cutoff distance of 10.0 Å was applied as defined in the Garofalini model.[23] The proton transfer update criterion ρ was set to the recommended value of 0.59[42].

The Berendsen thermostat and manostat[49] were employed to maintain constant temperature and pressure, respectively. The relaxation times were set to τ_T = 0.1 ps for temperature and τ_p = 0.5 ps for pressure. A previous investigation of PT events employing the Garofalini model in both the NVE and the NpT ensemble resulted in very similar proton hopping frequencies and diffusion coefficients[42]. This finding can be explained by the fact that the diffusion coefficient is determined in the so-called long time limit, averaging over a large number of evaluation windows. Thermal and pressure oscillations introduced by a thermostat/manostat algorithm occur on a much shorter timescale, thereby being averaged by the analysis procedure. On the other hand, it is important that the simulations performed with different parametrizations are executed at identical conditions, hence the latter ensemble has been chosen. Otherwise there is a risk of differences of the diffusivity observed for the different parameter sets being a result of varying thermal and pressure conditions stemming from the artificial isolation of the system in an NVE setup.

In order to sufficiently relax and equilibrate the systems, they were minimized via MD to 1 K and subsequently, over the course of 75 000 MD steps, heated to 298.15 K. Afterwards, the systems were pressurized at 1 atm. Another 3.15 million MD equilibration steps were performed to relax all tension, which might have been introduced by the setup procedure. The final cubic simulation boxes had an edge length of about 31 Å. Each simulation performed after this equilibration phase

used the same starting structure in case of light and deuterated solution.

After changing the parameters according to table 1 the systems were again equilibrated for 500 000 MD steps (100 ps) to enable further relaxation of the systems according to changed potential. Subsequently, sampling was performed for 2.5 million MD steps (0.5 ns). To tightly monitor all occurring proton transfer events data sampling was performed every fifth MD step, leading to trajectory file sizes of approximately 65 GB per parameter set.

Analysis

In order to adequately analyze the proton transfer behavior a locator particle approach, as described by Hofer et al.[42], was employed. By following the path of this locator particle an accurate estimate of the diffusion coefficient D can be obtained, using the Einstein relation given as

$$D = \frac{1}{2d} \lim_{t \to \infty} \frac{\langle \|\mathbf{r}_t - \mathbf{r}_0\|^2 \rangle}{t} \tag{6}$$

where d is the dimensionality of the system, $\mathbf{r}_t$ and $\mathbf{r}_0$ correspond to the position of the locator particle at time t and the time origin, respectively. The correlation length was set to 2000 frames (2 ps) using the last half of the correlation (1 ps) for the regression to determine the diffusion coefficient.

The associated average proton hopping rate h is obtained as the quotient of the number of registered exchange events and the simulation time. The corresponding average lifetime of the proton τ is given as the inverse of h.

Furthermore, structural properties of the systems were analyzed via radial (RDF) and angular distribution functions (ADF). The vibrational power spectra were evaluated by employing the velocity auto-correlation function (VACF) $C(t)$ and subsequent Fourier-transformation.

$$C(t) = \frac{\sum_{i}^{N_t} \sum_{j}^{N} \mathbf{v}_j(t_i)\mathbf{v}_j(t_i + t)}{\sum_{i}^{N_t} \sum_{j}^{N} \mathbf{v}_j(t_i)\mathbf{v}_j(t_i)} \quad (7)$$

N and N_t are the number of particles and the number of time origins t_i, respectively. v_j denotes a certain velocity component of particle j. The vibrational power spectrum was obtained employing a correlation length of 1000 frames (1 ps).

Results

Diffusive properties of the excess proton and deuteron

After 0.5 ns of simulation time proton transfer maps (PTMs) have been generated for the excess proton in each of the eight systems. Figure 3 depicts the PTMs obtained from the simulations using the different parametrization for HCl in light water. The y-axis denotes the index of the water molecule carrying the excess proton at a given timestep of the simulation. Vertical lines represent observed exchange events by connecting the molecular indices of the participating water molecules. In order not to miss a proton transfer occurring over the course of a simulation, a high output frequency of the order of 1 frame per fs is required. This explains the rather large disk requirements of 65 GB per simulation outlined earlier.

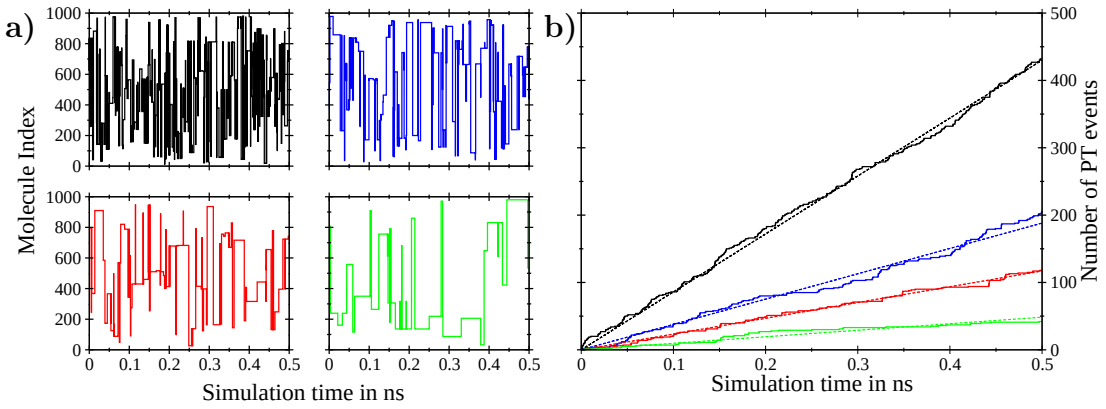

Figure 3: a) Proton transfer maps of the excess proton observed for different parametrizations of the three-body potential and b) associated number of registered proton transfer events. (Parameter sets A, B, C and D are colored black, blue, red and green, respectively.)

From figure 3a the strong influence of the different parametrizations on the number of PT events can be deduced, which are reduced from 432 to 42 when moving from set A to D. The use of the original parameters results in 119 PT reactions. The summation of the number of PT events occurring in the course of the simulations depicted in figure 3b shows a near-linear increase, demonstrating that the PTs are equally distributed over the respective trajectories.

Based on the PTMs it is possible to determine the average proton hopping frequency h as well as the corresponding diffusion coefficients D[42], which are summarized in table 2. The data highlight the expected correlation between the different parameter sets and the diffusive properties with a decrease of both h and D upon increase of the three–body cutoff distance r^0 when moving from set A to D. The hopping frequency h_H and diffusion coefficients D_H obtained for the original parameter set C agree well with those of an earlier investigation of an aqueous excess proton determined without the presence of a chloride counterion[42]. The associated average lifetime of the proton τ given as the inverse of the hopping frequency determined for the original set C in light water as 4.2 ps is in good

agreement with the estimations of Lockwood and Garofalini reporting an overall average lifetime of the excess proton (in the absence of chloride) of 4.5 ps [50].

The average proton hopping rate h_H obtained for parameter set A as 0.86 ps^{-1} agrees best with the value of 0.75 ps^{-1} derived from the mean residence time of an excess proton determined via NMR measurements[46] as approximately 1.33 ps[51]. Similarly, the diffusion coefficient D_H obtained for parameter set A as 0.87 $Å^2/ps$ is in good agreement with experimental estimations, reporting the diffusion coefficient of a proton in light water as 0.93 $Å^2/ps$[52] and 0.94 $Å^2/ps$[53]. Theoretical estimations assess its value to be 0.81 $Å^2/ps$[54] and 0.91 $Å^2/ps$[52]. Although the influence of nuclear quantum effects (NQEs) on the proton transfer properties has been reported as minor[34,51,55,56,57,58], its effects are not negligible. Since in this work all atoms have been treated as classical particles, simulations of an excess deuteron in heavy water (D_2O) have been conducted to estimate the diffusion coefficient without the influcene of NQEs. For the diffusion coefficient of a deuteron in heavy water experimental results yield a value of 0.62 $Å^2/ps$[59]. Other theoretical estimates report a value of 0.60 $Å^2/ps$[52]. Since the corresponding value determined in this work amounting to 0.59 $Å^2/ps$ is in excellent agreement with these values, the deviation between the value determined for the excess proton (0.87 $Å^2/ps$) and its experimental value (0.93 $Å^2/ps$) can be indeed attributed to the influence of nuclear quantum effects.

For the kinetic isotope effect given as the ratio of D_D and D_H experiment finds a value of 1.42[60]. Since the diffusion coefficients of the individual species obtained with parameter set A are in good agreement with experiment, a similar agreement is found for the respective kinetic isotope effect amounting to 1.46. The same applies to the kinetic isotope effects of the proton hopping rates h_D/h_H obtained as 1.40.

The observed diffusion data confirm the initial assessment that proton transfer

properties are highly sensitive to the parametrisation of the three–body potential. On the other hand, since great care was taken to maintain the equilibrium properties of the potential, other observables of the solutions can be expected to be largely unaffacted by the modified parameter set.

Set	h_H	h_D	k_{h_H/h_D}	D_H	D_D	k_{D_H/D_D}
A	0.864	0.618	1.40	0.869	0.594	1.46
B	0.412	0.336	1.22	0.519	0.453	1.15
C	0.238	0.150	1.58	0.357	0.284	1.26
D	0.084	0.058	1.45	0.310	0.236	1.31

Table 2: Average proton hopping rates h_H and h_D in ps^{-1} and diffusion coefficients D_H and D_D in $Å^2/ps$ for an excess proton and deuteron in light and heavy water as well as the respective kinetic isotope effects k_{h_H/h_D} and k_{D_H/D_D} obtained for parameter sets A to D.

To further analyze the dynamical properties of the different parametrizations, proton transfer time-correlation functions (TCFs) as introduced by Tuckerman *et al.*[61,62,63], which can be seen as analogues to the widely employed hydrogen bond correlation functions[64,65], have been evaluated. The continuous and intermittent PT correlation function $C_c(t)$ and $C_i(t)$ are defined as:

$$C_c(t) = \frac{\langle h(t_0)H(t_i)\rangle}{\langle h(t_0)\rangle} \tag{8}$$

$$C_i(t) = \frac{\langle h(t_0)h(t_i)\rangle}{\langle h(t_0)\rangle} \tag{9}$$

The population function $h(t)$ monitors whether an atom carrying a proton at time t_0 does so at time t_i, while $H(t)$ measures whether an atom continuously carries a proton in the time-period $[t_0, t_i]$. In case the condition is fulfilled, the population functions yield one, otherwise they return zero. The corresponding history-dependent continuous proton transfer correlation function $C_c(t)$ is a mea-

sure of the average proton-donor lifetime, which is obtained via integration of $C_c(t)$:

$$\tau_{exch} = \int_0^\infty C_c(t)dt \tag{10}$$

Furthermore, a double-exponential fit of $C_c(t)$ yields the respective slow and fast decay-times τ_s and τ_f.

$$C_c(t) \approx a_f e^{-\frac{t}{\tau_f}} + a_s e^{-\frac{t}{\tau_s}} \tag{11}$$

Sometimes double-exponential fitting is not possible, in which case only a single-exponential expression is used, yielding only the slow decay-time.

The intermittent proton transfer correlation function $C_i(t)$ on the other hand, gives the probability of an atom carrying a proton at the time origin t_0, as well as at a later time t_i, irrespective of any transfer events occurring during the period $[t_0,t_i]$. Using the parameters a_0, a_1 and a_2 determined via double-exponential fit of $C_i(t)$ (eqn. 12) the forward rate constant k_1^{PT} can be determined as[66]

$$C_i(t) \approx a_0 e^{-a_1 t} + (1 - a_0)e^{-a_2 t} \tag{12}$$

$$k_1^{PT} = a_1 a_0 + a_2(1 - a_0) \tag{13}$$

Tuckerman and coworkers have also discussed the influence of rattling events on proton transfer correlation functions[66]. It was shown that these short-time proton transfer events should be excluded from the analysis, since they do not contribute to the overall net displacement of charge. Excluding them leads to time scales and rates associated entirely with the actual charge transport process[61]. Since these kind of short-time fluctuations are not registered as successful PT events due to

the use of a threshold ratio $\bar{\rho}$[42], data obtained from the proton transfer mapping presented in this paper are direcetly comparable to the results of Tuckerman *et al.* [61], which are summarised in table 3.

		τ_{exch}	$\frac{1}{k_1^{PT}}$	τ_f	τ_s	a_s	
D^+	PW91	1.24	1.00	0.36	1.85	0.60	Ref [61]
	BLYP	1.66	1.68	-	1.75	1.00	
	HCTH	1.70	1.57	0.15	1.88	0.93	
H^+	set A	1.69	1.38	0.52	2.00	0.790	this work
	set B	4.06	2.98	0.35	4.31	0.939	
	set C	5.17	4.56	0.035	6.11	1.00	
	set D	14.4	18.5	0.031	15.4	1.00	
D^+	set A	2.07	1.83	0.328	2.20	0.928	
	set B	4.56	4.15	0.485	4.78	0.951	
	set C	9.22	8.70	0.008	10.2	1.00	
	set D	18.3	11.3	-	19.3	1.00	

Table 3: Relaxation times and inverse rates in ps obtained for the different parameter sets.

It can be seen that τ_{exch}, $1/k_1^{PT}$ and τ_s decrease when moving from parameter set D to A, whereas τ_f shows an increasing trend. Values for τ_{exch} and τ_s determined for H^+ with the original parameter set C as 5.17 and 6.11 ps are in good agreement with results presented by Garofalini yielding 4.4 and 6.5 ps[50], respectively.

Use of the recommended parametrization A on the other hand yields data in very good agreement with results obtained for D^+ using Car-Parrinello molecular dynamics simulations executed at the PW91, BLYP and HCTH levels[61], respectively. The value determined for τ_{exch} being 2.07 ps agrees best with the value of 1.70 ps determined using the HCTH functional, while the inverse of the forward rate constant $1/k_1^{PT}$ of 1.83 ps closely matches the value of 1.68 ps determined using the BLYP functional. Although the slow decay time τ_s is slightly higher than the reported values, the fast decay time τ_f is in excellent agreement with the

corresponding results obtained at the PW91 level. This comparison of the simulation data with results obtained from the computationally much more demanding CP-MD simulations further confirms the improved dynamical properties of the adjusted parameter set A.

Influence on structural and dynamical properties of the solution

To monitor the influence of the new parameter set on the equilibrium properties of the solution, the corresponding O–O, O–H and H–H radial distribution functions (RDFs) as well as the intramolecular H-O-H angular distribution function (ADF) were calculated for optimized and original parameter sets A and C and have been compared (*cf.* fig. 4). This data confirm that the impact of the proposed parameters on the structural properties of the light and deuterated solution is marginal. Only for the peak intensities minor changes are observed, while the positions of maxima and minima coincide in all cases. The intensities of the O-O distributions decrease when changing from set C to A. All other distributions show an opposite trend. These observations can be explained by considering the modifications made to the screening function displaying a steeper slope near the average O–H distance (*cf.* fig. 2). Thus, for O–H separations smaller than its equilibrium value of 0.985 Å, the effective force constant of the three-body potential is higher in case of the modified parameter set, resulting in a diminutive but noticeable narrowing of the H–H pair correlation and the associated H–O–H angle distribution. Similarly, the increased steepness of the slope leads to an increase of the repulsive forces $\mathbf{F}^{scr}$, resulting from the derivation of the screening functions, which explains the reduced intensity in case of the O–H distribution. The broadening of the H-O-H and O-H distributions resulting from the modified parameter set implies an increased flexibility of intramolecular degrees of freedom. This on the other hand

promotes the formation of intermolecular hydrogen bonds, which is inline with the observed increase of the O–O pair distribution. Although the screening functions have been parametrized to yield identical values at the O–H equilibrium distance, the respective differences of the peak intensities are less than 1% and can thus be safely considered negligible.

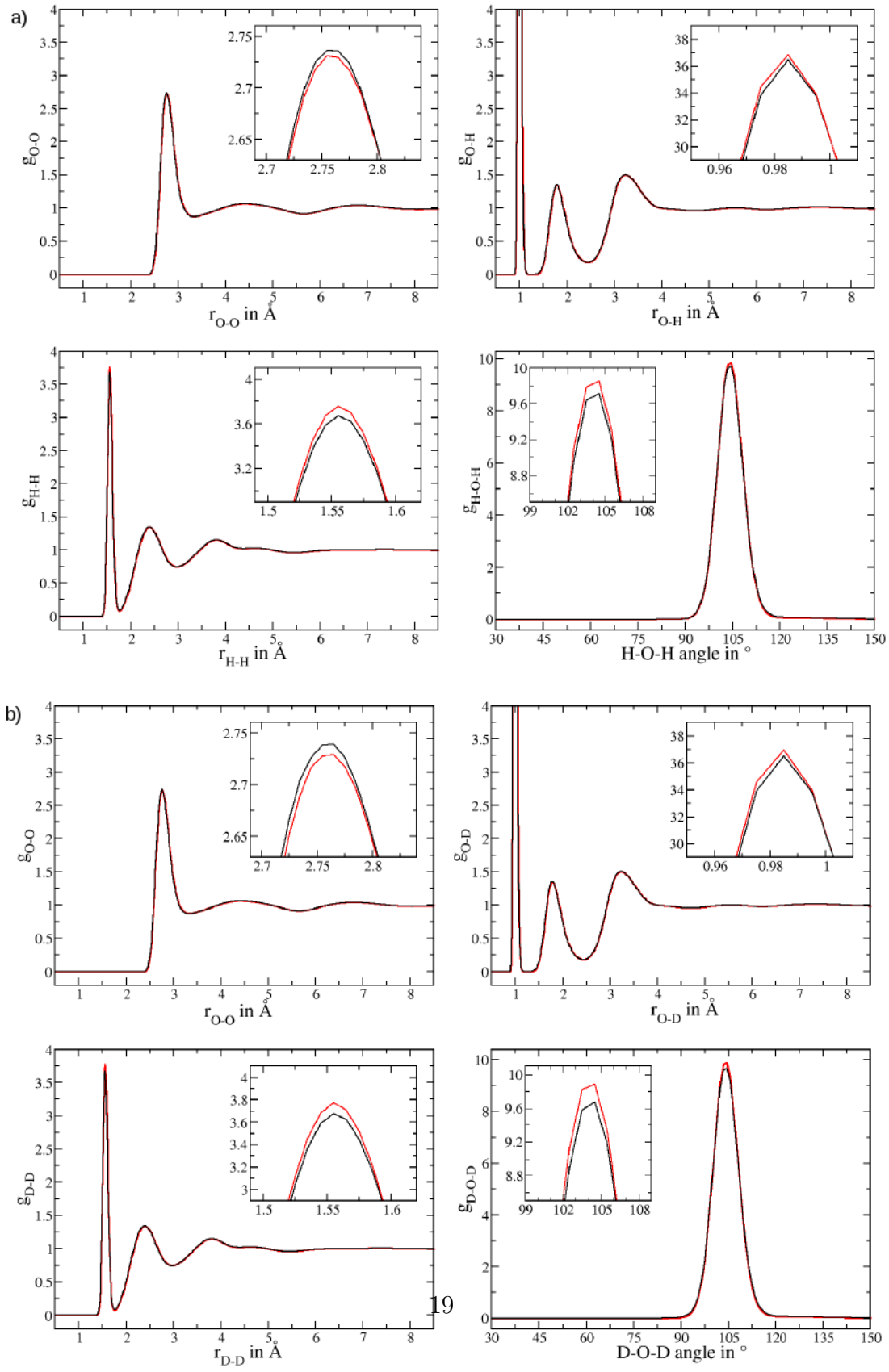

Figure 4: Pair and angular distribution functions obtained for a) HCl in H_2O and b) DCl in D_2O employing the modified (black) and original (red) three-body parameter sets A and C, respectively.

This conclusion is underlined by the average densities obtained for the different parameter sets being in excellent agreement with each other (see table 4), thus further demonstrating the minor influence of the re-parametrization on the properties of the solutions.

Set	HCl/H_2O	DCl/D_2O
A	1.004	1.116
C	1.004	1.114

Table 4: Average densities in kg/dm^3 for aqueous hydrochloric acid in light and heavy water employing the modified and original three-body parameter sets A and C, respectively.

In addition to the analysis of structural data, dynamical properties of the solutions have been determined. Figure 5 depicts a comparison of the vibrational power spectra obtained via Fourier transformation of the velocity auto-correlation function. The bending modes show the largest differences between the parameter sets, with frequency shifts of 16 cm^{-1} for light water and 14 cm^{-1} in the deuterated case along with a decrease of the peak intensity resulting from a broadening of the peak. The change in frequency demonstrates that although the screening functions of the three–body potential adopt the same value at the O–H equilibrium distance, the varying slopes of the different parametrizations result in different average force constants of the H-O-H bending mode in the course of the simulations. Since the increased steepness of the modified parameter set results in a broader fluctuation of the effective angular force constant, a larger number of frequencies occurs, explaining the broadening of the peak along with the decrease of its intensity.

While the change in intensity of the stretching modes is less pronounced than in case of the bending vibration, an even smaller magnitude of the shift in frequency of 8 cm^{-1} for light water and 9 cm^{-1} in the deuterated case is observed. Again the varying slopes of the screening functions may explain these deviations. The

increased steepness in case of parameter set A results in a slightly lowered curvature at the O–H equilibrium distance (*cf.* fig. S1). Since the derivative of the screening functions results in forces parallel to the O-H bond, the reduction of the curvature compared to the original set results in a slight red-shift of the maximum of the stretching mode. In case of the rotational modes no noticeable difference between the parameter sets can be observed.

As a final test the average diffusion coefficients of all oxygen atoms obtained for the different parameter sets have been determined, being again in good agreement with each other (*cf.* tab. 5). The observed deviations may be explained by the strongly increased diffusivity of the excess proton, which can be expected to influence the diffusive properties of all other atoms in the system.

Set	HCl/H_2O	DCl/D_2O
A	0.259	0.231
C	0.264	0.238

Table 5: Average diffusion coefficient of oxygen atoms in $Å^2/ps$ for aqueous hydrochloric acid in light and heavy water employing the modified and original three-body parameter sets A and C, respectively.

Since set A displays the largest deviation from the original parametrization, structural and dynamical data obtained via sets B and D show an even better agreement when compared to results of set C (data not shown).

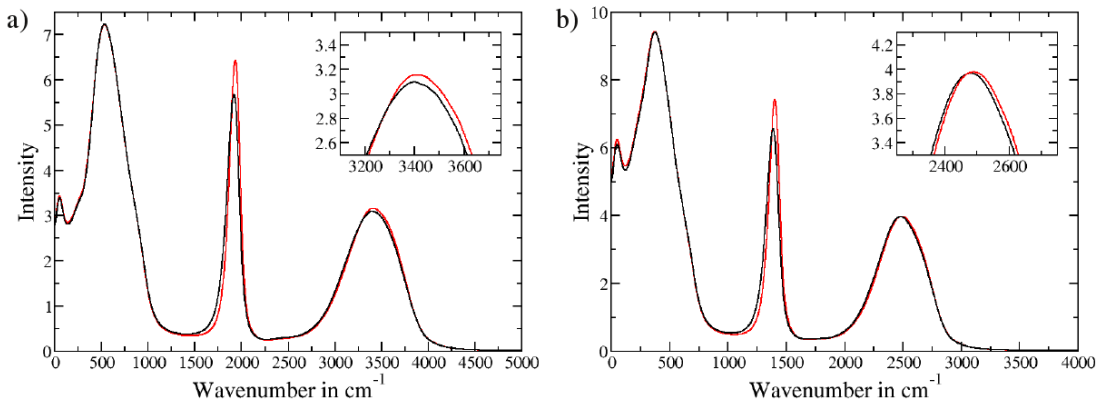

Figure 5: Vibrational spectrum of aqueous hydrochloric acid in a) light and b) deuterated solution, employing the modified (black) and original (red) three-body parameter sets A and C, respectively.

Conclusion

In this work the properties of the dissociative water potential developed by Garofalini and coworkers were closely examined with special focus on the proton transfer dynamics. By carefully analyzing the pairwise screening functions of the three-body interaction, a strategy to selectively adjust the diffusive properties of an excess proton via a simultaneous change of the exponential factor and the three-body cutoff distance was formulated. As a consequence the transferring proton is subject to significantly altered intermolecular forces, whereas the potential energy landscape for molecular species such as H_2O, OH^- and H_3O^+ remains to a large extend unaffected by the re-parametrization.

The best parametrization used in this study was identified as set A, leading to significant improvements of the diffusion coefficient and the proton hopping rate as well as the respective kinetic isotope effects. In particular the agreement of D obtained for the deuterated system with experimental data highlights the

improved accuracy of the adjusted parameter set, since in this case the influence of nuclear quantum effects is negligible. Data obtained via proton transfer correlation functions demonstrate that the suggested parameter set yields data in excellent agreement with results obtained via Car-Parrinello molecular dynamics simulations performed at PW91, BLYP and HCTC levels.

Analysis of structural data via pair and angle distribution functions, as well as the overall density and dynamical properties, such as the vibrational power spectra and oxygen diffusion coefficients, confirmed the assessment of the diffusive properties of the excess proton being sensitive to the three–body parameters. At the same time structure and dynamics of the solutions are reproduced in very good agreement compared to the original parameter set.

Based on the obtained data the parametrization strategy could be optimized even further, *e.g.* by ensuring that the average effective force constant of the three–body potential occurring throughout an MD simulation coincides with that of the original set. However, since all distances in the pair distributions are exactly reproduced by the newly proposed parameter set and the deviations observed in case of the vibrational frequencies are less than one percent, the performance of the modified parameters to predict structural and vibrational data can be considered as equivalent to the original set.

The proposed alterations will not only contribute to a better understanding of the dynamic properties of aqueous solutions, but provide valuable insight into the sensitivity of reactive properties in dissociative force field formulations.

A further important question is focused on the performance of the proposed parameter set to describe the diffusive properties of the proton hole in hydroxide containing systems. Since in this case nuclear quantum effects[55,56] are known to be more prominent than for the hydrated excess proton, these effects have to be adequately taken into account. In this context the importance to investigate

systems with and without deuteration is clearly visible. Due to the chemical similarity of hydrogen and deuterium they exhibit the same potential, both in quantum mechanical approaches as well as in empirical potentials. Therefore deuerated systems can be described with the same interaction potential as their hydrogenated counterparts. Since nuclear quantum effects are strongly diminished in case of deuterium, investigations of proton transfer phenomena via simulation as well as experiment should be carried out with and without deuteration. That way it is possible to compare data from different sources without any uncertainty resulting from the neglect of NQEs. The results and discussions presented in this work will provide a valuable starting point for such future investigations.

Acknowledgment

Financial support by the Tyrolean Science Fund (TWF) is gratefully acknowledged (Project J 2833). This work was supported by the Austrian Ministry of Science BMWF as part of the Konjunkturpaket II of the Focal Point Scientific Computing at the University of Innsbruck.

References

[1] Nobel Prize in Chemistry 2013.

[2] Szabo, A.; Ostlund, N. *Modern Quantum Chemistry: Introduction to Advanced Electronic Structure Theory.* Dover Pubn. Inc., 1.rev. edition 1996.

[3] Helgaker, T.; Jørgensen, P.; Olsen, J. *Molecular Electronic-Structure Theory.* Wiley 2000.

[4] Koch, W.; Holthausen, M. *A Chemist's Guide to Density Functional Theory.* 1.repr. Wiley-VCH, 2nd edition 2002.

[5] Leach, A. R. *Molecular Modelling*, volume 2nd Edition. Prentice-Hall, Harlow 2001.

[6] Jensen, F. *Introduction to Computational Chemistry.* JW, 2. edition December 2011.

[7] Cramer, C. J. *Essentials of Computational Chemistry.* Wiley, West Sussex 2002.

[8] Jorgensen, W. L.; Tirado-Rives, J. *J. Am. Chem. Soc.* **1988**, *110*, 1657.

[9] Cornell, W. D.; Cieplak, P.; Bayly, C. I.; Gould, I. R.; Merz Jr, K. M.; Ferguson, D. M.; Spellmeyer, D. C.; Fox, T.; Caldwell, J. W.; Kollman, P. A. *J. Am. Chem. Soc.* **1995**, *117*, 5179.

[10] Jorgensen, W. L.; Maxwell, D. S.; Tirado-Rives, J. *J. Am. Chem. Soc.* **1996**, *118*, 11225.

[11] MacKerell Jr., A. D.; Banavali, N.; Foloppe, N. *Biopolymers* **2000**, *56*, 257.

[12] Duan, Y.; Wu, C.; Chowdhury, S.; Lee, M. C.; Xiong, G.; Zhang, W.; Yang, R.; Cieplak, P.; Luo, R.; Lee, T.; Caldwell, J.; Wang, J.; Kollman, P. *J. Comput. Chem.* **2003**, *24*, 1999.

[13] Ponder, J. W.; Case, D. A. *Adv. Protein Chem* **2003**, *66*, 27.

[14] Mackerell, A. D. *J. Comput. Chem.* **2004**, *25*, 1584.

[15] Cygan, R. R.; Liang, J.; Kalinichev, A. G. *J. Phys. Chem. B* **2004**, *108*(4), 1255.

[16] Maginn, E. J. *J. Phys.: Condens. Matter* **2009**, *21*(37), 373101.

[17] Borodin, O. *J. Phys. Chem. B* **2009**, *113*, 11463.

[18] Dommert, F.; Wendler, K.; Berger, R.; Delle, S.; Holm, C. *ChemPhysChem* **2012**, *13*, 1625.

[19] Lennard-Jones, J. E. *Proc. R. Soc. Lond. A* **1924**, *106*(738), 441 – 462.

[20] Lennard-Jones, J. E. *Proc. R. Soc. Lond. A* **1924**, *106*(738), 463 – 477.

[21] van Duin, A. C. T.; Dasgupta, S.; Lorant, F.; Goddard, W. A. *J. Phys. Chem. A* **2001**, *105*(41), 9396–9409.

[22] Hofmann, D. W.; Kuleshova, L.; D'Aguanno, B. *Chem. Phys. Lett.* **2007**, *448*(13), 138.

[23] Mahadevan, T. S.; Garofalini, S. H. *J. Phys. Chem. B* **2007**, *111*, 8919.

[24] Lammers, S.; Lutz, S.; Meuwly, M. *J. Comput. Chem.* **2008**, *29*(7), 1048.

[25] Rahman, A.; Stillinger, F. H.; Lemberg, H. L. *J. Chem. Phys.* **1975**, *63*, 5223.

[26] Stillinger, F. H. *Adv. Chem. Phys.* **1975**, *31*, 1.

[27] Stillinger, F. H.; Rahman, A. *J. Chem. Phys.* **1978**, *68*, 666.

[28] Billeter, S. R.; van Gunsteren, W. F. *Comp. Phys. Commun.* **1997**, *107*, 61.

[29] Billeter, S. R.; van Gunsteren, W. F. *J. Phys. Chem. A* **1998**, *102*, 4669.

[30] Ojamäe, L.; Shavitt, I.; Singer, S. *J. Chem. Phys.* **1998**, *10(F. H. Stillinger, Adv. Chem. Phys. 1975, 31, 1; D. C. Rapaport, Mol. Phys. 1983, 50, 1151)9*(13), 5547.

[31] Lee, S.; Rasaiah, J. *J. Chem. Phys* **2011**, *135*, 124505.

[32] Wolf, M.; Groenhof, G. *J. Comput. Chem.* **2014**, *35*(8), 657 – 671.

[33] Warshel, A.; Weiss, R. M. *J. Am. Chem. Soc.* **1980**, *102*, 6218.

[34] Sagnella, D. E.; Tuckerman, M. E. *J. Chem. Phys.* **1998**, *108*, 2072.

[35] Schmitt, U. W.; Voth, G. A. *J. Phys. Chem. B* **1998**, *102*, 5547.

[36] Vuilleumier, R.; Borgis, D. *J. Chem. Phys.* **1999**, *111*, 4251.

[37] Čuma, M.; Schmitt, U. W.; Voth, G. A. *J. Phys. Chem. A* **2001**, *105*, 2814.

[38] Brancato, G.; Tuckerman, M. E. *J. Chem. Phys.* **2005**, *122*, 224507.

[39] Wu, Y.; Chen, H.; Wang, F.; Paesani, F.; Voth, G. A. *J. Phys. Chem. B* **2008**, *112*, 467.

[40] Park, K.; Lin, W.; Paesani, F. *J. Phys. Chem. B* **2012**, *116*, 343.

[41] Ufimtsev, I. S.; Kalinichev, A. G.; Todd, M. J.; Kirkpatrick, R. J. *Phys. Chem. Chem. Phys.* **2009**, *11*, 9420.

[42] Hofer, T.; Hitzenberger, M.; Randolf, B. *J. Chem. Theory Comput.* **2012**, *8*(10), 3586 – 3595.

[43] Canaval, L. R.; Lutz, O. M. D.; Weiss, A. K. H.; Huck, C. W.; Hofer, T. S. *Inorg. Chem.* **2014**, *8*, 3586.

[44] Roberts, N. K.; Northey, H. L. *J. Chem. Soc., Faraday Trans.* **1974**, *70*, 253.

[45] Pines, E.; Huppert, D.; Agmon, N. *J. Chem. Phys.* **1988**, *88*, 5620.

[46] Luz, Z.; Meiboom, S. *J. Am. Chem. Soc.* **1964**, *86*, 4768.

[47] Webb, M. B.; Garofalini, S. H.; Scherer, G. W. *J. Phys. Chem. B* **2009**, *113*, 9886.

[48] Wolf, D.; Keblinski, P.; Phillpot, S.; Eggebrecht, J. *J. Chem. Phys.* **1999**, *110*(17), 8254 – 8282.

[49] Bernedsen, H. J. C.; Postma, J. P. M.; van Gunsteren, W. F.; DiNolta, A.; Haak, J. R. *J. Chem. Phys.* **1984**, *81*(8), 3684 – 3692.

[50] Lockwood, G. K.; Garofalini, S. H. *J. Phys. Chem. B* **2013**, *117*, 4089.

[51] Wraight, C. A. *Biochim. Biophys. Acta* **2006**, *1757*, 886.

[52] Pines, E.; Huppert, D.; Agmon, N. *J. Chem. Phys.* **1988**, *88*(9), 5620 – 5632.

[53] Roberts, N.; Northey, H. *J. Chem. Soc., Faraday Trans. 1* **1972**, *68*, 1528 – 1532.

[54] Wraight, C. *Biochim. Biophys. Acta* **2006**, *1757*, 886 – 912.

[55] Tuckerman, M.; Marx, D.; Klein, M.; Parrinello, M. *Science* **1997**, *275*, 817.

[56] Marx, D.; Tuckerman, M. E.; Hutter, J.; Parrinello, M. *Nature* **1999**, *397*, 601.

[57] Marx, D. *ChemPhysChem* **2006**, *7*, 1848.

[58] Fifen, J.; Dhaouadi, Z.; Nsangou, M. *J. Phys. Chem. A* **2014**, *118*(46), 11090 – 11097.

[59] Roberts, N.; Northey, H. *J. Chem. Soc., Faraday Trans. 1* **1974**, *70(F. H. Stillinger, Adv. Chem. Phys. 1975, 31, 1; D. C. Rapaport, Mol. Phys. 1983, 50, 1151)*, 253 – 262.

[60] Conway, B.; Bockris, J.; Linton, H. *J. Chem. Phys.* **1956**, *24*(4), 834 – 850.

[61] Tuckerman, M.; Chandra, A.; Marx, D. *J. Chem. Phys.* **2010**, *133*(12), 124108.

[62] Chandra, A.; Tuckerman, M.; Marx, D. *Phys. Rev. Lett.* **2007**, *99*(14), 145901.

[63] Berkelbach, T.; Lee, H.-S.; Tuckerman, M. *Phys. Rev. Lett.* **2009**, *103*(23), 238302.

[64] Stillinger, F. *Adv. Chem. Phys* **1975**, *31*, 1 – 101.

[65] Rapaport, D. C. *Mol. Phys.* **1983**, *50*, 1151.

[66] Marrone, J. A.; Haslinger, K. E.; Tuckerman, M. E. *J. Phys. Chem. B* **2006**, *110*(12), 3712.